

The ALHAMBRA survey: Discovery of a faint QSO at $z = 5.41$ (Research Note)

I. Matute¹, J. Masegosa¹, I. Márquez¹, A. Fernández-Soto^{2,3}, C. Husillos¹, A. del Olmo¹, J. Perea¹, M. Pović¹, B. Ascaso¹, E. J. Alfaro¹, M. Moles^{1,4}, J. A. L. Aguerri⁵, T. Aparicio-Villegas⁶, N. Benítez¹, T. Broadhurst⁷, J. Cabrera-Cano^{1,8}, F. J. Castander⁹, J. Cepa^{5,10}, M. Cerviño^{1,5}, D. Cristóbal-Hornillos^{1,4}, L. Infante¹⁰, R. M. González Delgado¹, V. J. Martínez^{3,12,13}, A. Molino¹, F. Prada¹, and J. M. Quintana¹

¹ Instituto de Astrofísica de Andalucía (CSIC), Glorieta de la Astronomía s/n, E-18008 Granada, Spain

e-mail: matute, isabel, pepa, cesar, chony, jaime, mpovic, emilio, benitez, mcs, rosa, amb, fprada, quintana@iaa.es

² Instituto de Física de Cantabria (CSIC-UC), E-39005, Santander, Spain; fsoto@ifca.unican.es

³ Unidad Asociada Observatori Astronòmic (IFCA - Universitat de València), Valencia, Spain

⁴ Centro de Estudios de Física del Cosmos de Aragón (CEFCA), E-44001 Teruel, Spain; moles, dch@cefca.es

⁵ Instituto de Astrofísica de Canarias, La Laguna, Tenerife, Spain; jalfonso@iac.es

⁶ Observatorio Nacional-MCT, CEP 20921-400, Rio de Janeiro-RJ, Brazil; villegas@on.br

⁷ School of Physics and Astronomy, Tel Aviv University, Israel; tjb@wise.tau.ac.il

⁸ Facultad de Física. Departamento de Física Atómica, Molecular y Nuclear. Universidad de Sevilla, Sevilla, Spain; jcc-famn@us.es

⁹ Institut de Ciències de l'Espai. IEEC-CSIC, Barcelona, Spain; fjc@ieec.fcr.es

¹⁰ Departamento de Astrofísica, Facultad de Física, Universidad de la Laguna, Spain; jcn@iac.es

¹¹ Departamento de Astronomía, Pontificia Universidad Católica, Santiago, Chile; linfante@astro.puc.cl

¹² Departament d'Astronomia i Astrofísica, Universitat de València, Valencia, Spain; vicent.martinez@uv.es

¹³ Observatori Astronòmic de la Universitat de València, Valencia, Spain

Received May ??, 2013; accepted July 12, 2013

ABSTRACT

Aims. We aim to illustrate the potentiality of the Advanced Large, Homogeneous Area, Medium-Band Redshift Astronomical (ALHAMBRA) survey to investigate the high redshift universe through the detection of quasi stellar objects (QSOs) at redshifts larger than 5.

Methods. We searched for QSOs candidates at high redshift by fitting an extensive library of spectral energy distributions—including active and non-active galaxy templates as well as stars—to the photometric database of the ALHAMBRA survey (composed of 20 optical medium-band plus the 3 broad-band *JHK*, near-IR filters).

Results. Our selection over ≈ 1 square degree of ALHAMBRA data ($\sim 1/4$ of the total area covered by the survey), combined with GTC/OSIRIS spectroscopy, has yielded the identification of an optically faint QSO at very high redshift ($z = 5.41$). The QSO has an absolute magnitude of ~ -24 at the 1450Å continuum, a bolometric luminosity of $\approx 2 \times 10^{46}$ erg s⁻¹ and an estimated black hole mass of $\approx 10^8 M_{\odot}$. This QSO adds itself to a reduced number of known UV faint sources at these redshifts. The preliminary derived space density is compatible with the most recent determinations of the high- z QSO luminosity functions (QLF). This new detection shows how ALHAMBRA, as well as forthcoming well designed photometric surveys, can provide a wealth of information on the origin and early evolution of this kind of objects.

Key words. cosmology: Observations – galaxies: active – galaxies: distances and redshifts galaxies: evolution – galaxies: high-redshift – quasars: general

1. Introduction

It is now widely accepted that the release of gravitational energy, as matter falls into a supermassive black hole ($\sim 10^{6-9} M_{\odot}$; SMBH), is the main generation mechanism for the high luminosities observed in AGN. Inside the variety of the AGN family, quasi-stellar objects (quasars or QSOs) are the fraction that shows particularly high intrinsic luminosities that allow them to be detected over very large distances. Consequently, QSOs provide a way to peer into the physical conditions of an early universe and study the history of the QSOs and their host galaxy interaction over cosmic time. The largest samples of known QSOs are provided by the optical spectroscopic surveys carried out over thousands of sq. degrees of sky (e.g. SDSS and the 2dF QSO survey, 2QZ). These surveys secure tens of thousand of

QSO detections and are able to derive detailed luminosity functions up to $z \sim 3 - 4$ (e.g., Richards et al. 2006b; Siana et al. 2008; Croom et al. 2009; Ross et al. 2012) in the form of double power-laws with a characteristic luminosity (M^*) and faint and bright slopes (α and β for $M > M^*$ and $M < M^*$ respectively). The situation at very high- z ($z \geq 5$) is quite different. At these redshifts, most of the identified QSOs (~ 300 objects above $z \sim 5$ and ~ 40 at $z > 6$) sample only the brightest end of the QSO luminosity function (QLF; Wolf et al. 2003; Fan et al. 2006; Jiang et al. 2009; Willott et al. 2010b; McGreer et al. 2012; Pâris et al. 2012). Over the redshift range $z = [5.0, 6.2]$, less than 10% of the known QSOs (23 objects; Mahabal et al. 2005; Jiang et al. 2009; Willott et al. 2010b; Masters et al. 2012; McGreer et al. 2012) sample the faint part of the QLF ($M_{1450} > -25$ where M_{1450} is the monochromatic luminosity at rest frame 1450 Å). This not

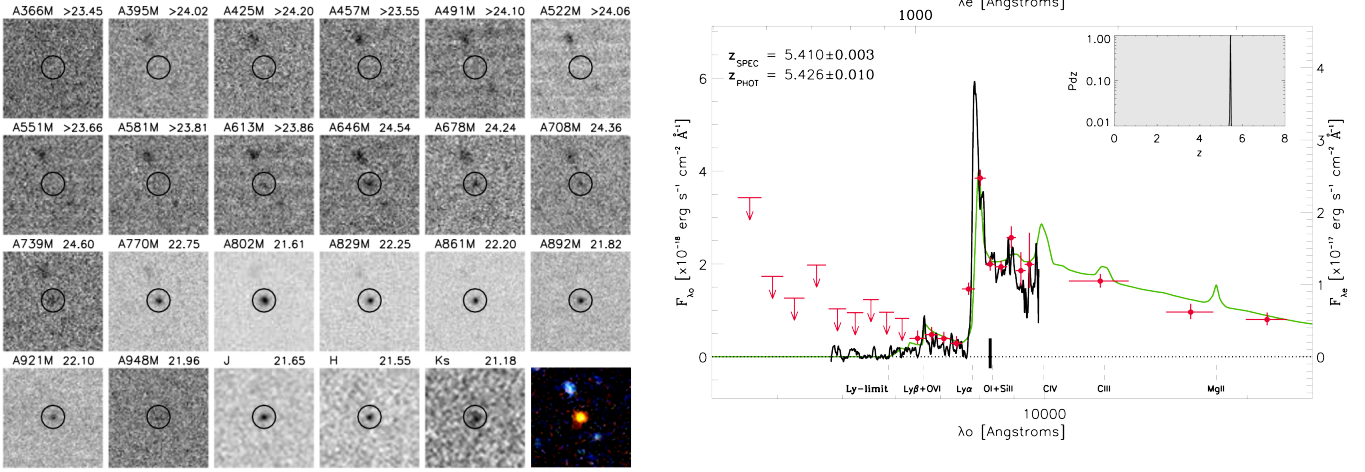


Fig. 1. *Left*) Cutouts ($15'' \times 15''$) in all the ALHAMBRA optical/NIR filters for the discovered QSO (highlighted by an open circle). Above each cutout we indicate the filter name and measured magnitude (or $5\text{-}\sigma$ lower limit). The final image is a colour composite of all bands, where the contrast has been increased in order to make all objects clearly visible. Images are oriented with north up and east to the left. *Right*) Optical–NIR spectral energy distribution of the discovered QSO. ALHAMBRA photometric detections are represented as circles with associated error bars (arrows indicate the 5σ upper limits). The reference magnitude in the m_{330} filter is indicated by a vertical thick line. The best photo- z template solution (QSO with optical slope index $\alpha = -0.25$ at $z_{\text{PHOT}} = 5.426 \pm 0.010$) is shown as a green line while the OSIRIS/GTC spectrum (smoothed with a 7 pixel box) is shown as a thick black line, with the redshift probability function (Pd z) in the inset. The agreement found between the spectro- z and the photo- z is remarkable. The most important emission lines for QSOs at the redshift of the source are also indicated.

only restrains our knowledge of the true number of faint QSOs at these redshifts but also severely hampers the derived accuracy of the overall QLF (given the high correlation between the LF parameters). This uncertainty in the high- z QLF limits our capability to answer some important cosmological questions such as the contribution of QSOs to the epoch of re-ionization (Fan et al. 2006; Dunkley et al. 2009; Schroeder et al. 2013), the formation of SMBHs within the first billion years of the universe and its challenge to models of galaxy formation, BH formation, and BH growth (Di Matteo et al. 2005; Hopkins et al. 2010; Melia 2013; Khandai et al. 2012)

The optical selection of QSOs has been performed mainly with follow-up spectroscopic observations of colour–colour selected candidates (e.g., Croom et al. 2004; Richards et al. 2002a; Pâris et al. 2012; McGreer et al. 2012; Palanque-Delabrouille et al. 2013), using slitless or prism spectroscopic surveys and through poorly efficient flux–limited spectroscopic surveys (e.g. VIMOS–VLT Deep Survey, Bongiorno et al. 2007). The novel photometric survey definition by COMBO–17 (Wolf et al. 2003) introduced for the first time a highly efficient selection criteria for QSOs with photometric redshift (photo- z) estimates with precisions of $\Delta z/(1+z) \sim 0.03$. Following the same philosophy, the Advanced Large, Homogeneous Area, Medium-Band Redshift Astronomical (ALHAMBRA¹) survey aims at probing a large cosmological fraction of the universe with a deep and wide catalogue of extragalactic sources with highly accurate photometry (Moles et al. 2008). The survey actually covers $\sim 4 \text{ deg}^2$ over eight different regions of sky and provides a photometric dataset over 20 contiguous, equal-width, non-overlapping, medium-band optical filters (3500 – 9700 Å) plus the 3 standard broad-band NIR filters JHK_S (Benítez et al. 2009; Aparicio Villegas et al. 2010). The capabilities of the ALHAMBRA survey to select and classify extragalactic sources with its *very-low-resolution-spectra* have been explored for

galaxies and AGN by Molino et al. (2013, submitted) and Matute et al. (2012) respectively. The photometric redshift precision achieved is $\Delta z/(1+z) \sim 0.011$ and 0.009 for galaxies and AGNs, respectively. A morphological classification for more than 20000 ALHAMBRA galaxies (with photo- $z < 1.3$) has been recently derived by Pović et al. (2013, submitted).

We present here the discovery of a UV-optically faint QSO at a redshift of 5.41 from the ALHAMBRA photometric survey. The selection criteria and spectroscopic observations are described in §2 and §3 respectively, while §4 presents the general properties of the QSO. The significance of our discovery is discussed in §4 and the conclusions are summarised in §5. Throughout this paper we assume a Λ CDM cosmology with $H_0 = 73 \text{ km s}^{-1} \text{ Mpc}^{-3}$, $\Omega_\Lambda = 0.73$, and $\Omega_M = 0.27$. Unless otherwise specified, all magnitudes are given in the AB system.

2. High- z QSOs candidates

Optical i -dropouts have proven useful in detecting high- z QSO (e.g., Fan et al. 2001, based on SDSS photometry). Unfortunately, the i -dropouts and broad-band colours of a $z \sim 5$ –6 QSO can look very similar to those of evolved/passive galaxies at $z \sim 1$ or of local red giants and super-giants. Matute et al. (2012) have shown that using the 23 bands of the ALHAMBRA photometric catalogue it is possible to efficiently classify an important fraction ($\sim 90\%$) of the $z = [0, 3]$ BLAGN/QSO population and measure highly accurate photometric redshifts.

We have applied the methodology described by Matute et al. (2012) to the search for high- z ($z > 5$) QSOs using the ALHAMBRA photometric database. The candidates were selected over $\approx 1 \text{ deg}^2$ in the two ALHAMBRA fields (out of eight; ALH-2/DEEP2 and ALH-8/SDSS) observable from the Roque de los Muchachos observatory in La Palma during the 2011B semester according to the following criteria: *i*) located in the fully exposed areas of the images and in regions not contaminated by bright sources flux or artifacts (e.g., spikes), *ii*) detected

¹ <http://www.alhambrasurvey.com>

Table 1. Properties of the quasar ALH023002+004647.

ALH-Field	ALH-2 (DEEP2)	(i)
R.A. (J2000)	02 ^{hh} 30 ^{mm} 02.27 ^{ss}	(ii)
DEC. (J2000)	+00 ^{dd} 46' 46.8''	(iii)
m_{830}	22.25 ± 0.08	(iv)
z_{PHOT}	5.426 ± 0.014	(v)
Best Fit SED	qso_0.25 (model #42)	(vi)
Best Fit $E(B - V)$	0.08	(vii)
Best Fit Ext. Law	SMC	(viii)
z_{SPEC}	5.410 ± 0.003	(ix)
EW(Ly α)	86	(x)
f_{1450}	1.388×10^{-17}	(xi)
M_{1450}	-24.07 ± 0.20	(xii)
L_{bol}	$46.28^{+0.19}_{-0.35}$	(xiii)
M_{BH}	$(1.52 \pm 0.83) \times 10^8$	(xiv)
α_O	0.25	(xv)

Notes. (i) ALHAMBRA field name; (ii,iii) Object coordinates; (iv) Observed magnitude in the ALHAMBRA A830M filter; (v, vi, vii, viii) Derived photo- z , template, intrinsic extinction and extinction law from the best fit to the ALHAMBRA photometry (for details see Matute et al. 2012); (ix) Spectroscopic redshift; (x) Rest-frame Ly α equivalent width (\AA) from our modelisation of the spectrum continuum and emission lines (see §4.5); (xi) Rest-frame monochromatic flux at 1450 \AA in units of $\text{erg s}^{-1} \text{cm}^{-2} \text{\AA}^{-1}$; (xii) Absolute magnitude at 1450 \AA ; (xiii) \log_{10} of the bolometric luminosity [erg s^{-1}]; (xiv) Black hole mass (M_{\odot}) assuming it radiates at the Eddington limit; (xv) Optical continuum power law index ($f \propto \nu^{-\alpha}$).

(at least) in the three NIR bands and the four reddest optical² filters and *iii*) having a best fit template of a BLAGN/QSO (templates numbers 29 to 59 in Matute et al. 2012), and photo- $z \geq 5$ with a probability³ at the selected redshift $> 50\%$. As a result of the spectroscopic follow-up of one of the highest probability candidates, we report the discovery and basic properties of ALH023002+004647, a low luminosity and very high redshift QSO. The *left* panel of Fig.1 shows the ALH023002+004647 cutouts of the 23 ALHAMBRA filters plus a colour composite.

3. Observations and Data Reduction

A pilot program, containing ALH023002+004647, was approved and observed with the OSIRIS⁴ spectrograph at the 10-meter GTC telescope located at the Observatorio del Roque de los Muchachos in La Palma. Since only a redshift confirmation and rough spectral classification was required, we used the low-resolution red grism R300R (with a resolution of 327 and a wavelength coverage from 5000 \AA to 10000 \AA) with a slit width of 1.2'' and a 2x2 on-chip binning. The observations of our candidates were carried out during September and November 2011 (period 2011B) under spectroscopic conditions.

The reduction process made use of standard IRAF/PyRAF facilities. Wavelength calibration was carried out by comparison with exposures of HgAr, Xe and Ne lamps. We used the 5577 \AA [O I] sky emission line to correct (applying a rigid shift) for the small offsets that can be introduced by instrument flexures. Relative flux calibration was carried out by observations of the spectrophotometric standard stars G158-100 and GRW708247.

² Notice that this implies the detection of flux at $8450 < \lambda < 9630 \text{\AA}$, which induces for this sample an upper limit on the redshift $z \lesssim 6$ and a photometric upper limit $m_z \lesssim 22.5$.

³ The photometric redshift code *LePhare* provides for each source the normalized probability distribution over redshift (Pd z), i.e. at each z (based on the photometry quality, the SED library and parameters assumptions) Pd z gives the probability that it is the correct one.

⁴ <http://www.gtc.iac.es/en/pages/instrumentation/osiris.php>

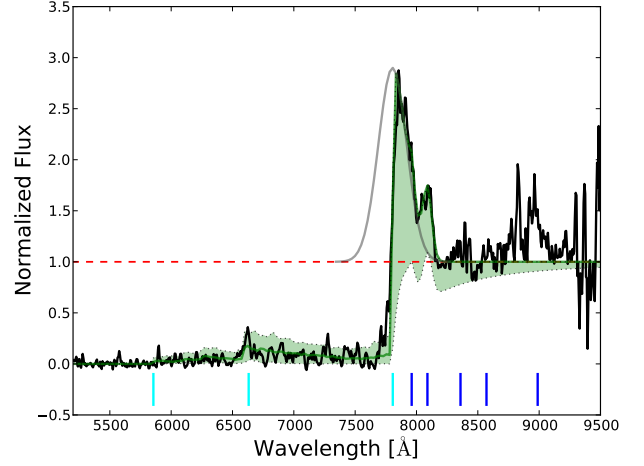


Fig. 2. Modelisation of the observed spectrum divided by the fitted continuum (*black* line). The Ly α , N V, and Si II $\lambda 1260$ lines have been modeled with Gaussian profiles. The Gaussian fit to Ly α is shown in grey. The result of dividing the normalized continuum plus the modeled lines by the median absorption, as well as upper and lower 2- σ deviations, generated by simulating 100 IGM sightlines at the same redshift are shown as a *continuous* (median) and *dotted green* line (2- σ limits). Vertical cyan lines mark the positions of the Lyman limit, Ly β , and Ly α lines at the reference redshift. Blue vertical lines mark the expected positions of the N V $\lambda 1240$, Si II $\lambda 1260$, O I $\lambda 1302$, C II $\lambda 1335$, and (O IV+Si IV) $\lambda 1400$ emission lines at the same redshift.

Each of the four 1200 s exposures was reduced and flux calibrated independently and they were combined afterward. The final spectrum is the result of 4800 s on-source integration time at a resolution of 6.5 $\text{\AA}/\text{pixel}$ with a continuum S/N of 10 at 1450 \AA rest-frame. The spectrum after smoothing with a 7 pixel-wide boxcar filter is shown in the *right* panel of Fig. 1, together with the ALHAMBRA photometry and best-fit template model.

4. Properties of ALH023002+004647

The spectrum of ALH023002+004647 shows typical features of a high- z QSO spectrum with a very blue continuum and prominent emission from broad Ly α , N V, Ly β +O VI and the Si IV+O IV complex. The continuum blue-wards of Ly α is substantially reduced due to intervening clouds of neutral hydrogen present in the IGM at different redshifts along the line of sight (the Ly α forest). Nevertheless, the presence of a detectable flux blueward of Ly α is a clear sign that the universe was highly ionised at the rest-frame of the source.

Table 1 resumes the main characteristics of the identified QSO.

4.1. Redshift

We derived a preliminary spectroscopic redshift $z = 5.410 \pm 0.003$ based on the position of the O I + Si II emission line $\lambda 1302$. The observed wavelength of Ly β +O VI is compatible with this redshift.

An alternative approach for measuring the redshift, which allows to use the highly asymmetric Ly α + N V complex, consists in modelling the continuum and the strongest emission lines (Ly α , N V and Si II), together with a stochastic realisation of the

IGM absorption. The result of such an approach is shown in Figure 2. The continuum has been normalised as a power law of slope 2.5 (as $F_\lambda \propto \lambda^{-2.5}$). The emission lines have been modeled with single Gaussian profiles, at a common redshift $z = 5.42$ for Ly α and Nv, and $z = 5.41$ for SiII $\lambda 1260$. The FWHM of the fitted Ly α is ≈ 1600 km/s, well above the ≈ 1000 km/s limit offered by the instrumental resolution of the grating we used, and usual for this type of objects.

In order to include the effect of the IGM in the spectrum, we have generated 100 Ly α forest absorption spectra for lines of sight corresponding to the given redshift $z = 5.42$, using the technique presented in Fernández-Soto et al. (2003). These spectra are able to reproduce the average absorption in the Ly α and Ly β regions, as well as the incidence of Lyman limit and Damped Ly α systems and the basic statistical properties of the absorption. For each pixel in the 100 resulting spectra we calculated the resulting median, 1σ and 2σ statistical absorption, and used them to generate the IGM absorption component over our continuum plus emission-line model.

As can be seen in Figure 2, the model perfectly reproduces the highly asymmetric (Ly α + Nv) profile, as well as the average observed flux in the Ly α and Ly β forest ranges. Only for the 2.5% densest IGM absorption sightlines the model would underestimate the data redward of Lyman α , and this is due to the putative presence, in those cases, of a strong Damped Ly α system at a redshift close to that of the quasar itself—a possibility which is clearly discarded by the data.

The Ly α redshift derived with this second method, $z = 5.420 \pm 0.005$, is in agreement with the O I + Si II estimate within the errors, but we cannot reject the possibility of an offset in the emission-line velocities, as observed in other quasar spectra. We find a small discrepancy between the redshift provided by Ly α and Nv, and the low-ionisation emission line. The disagreement is only of the order of ~ 500 km/s, but in a direction opposite to the expected one. We find the low ionisation lines—supposedly marking the real, systemic redshift—to be blueshifted with respect to our only clearly detected high ionisation line, Nv, which is in a position compatible with Lyman α .

As a comparison, Gaskell (1982) in his pioneering work found an offset of ≈ 600 km/s in the opposite direction to the one we find, whereas Richards et al. (2002b) and Shen et al. (2007), using large samples of quasars, found deviations of the same order, albeit with large scatter, covering from -500 out to 2000 km/s and beyond. Such scatter would, in fact, render the difference observed in ALH023002+004647 compatible with their extreme cases. However, we would need a better spectrum (particularly in terms of signal-to-noise ratio) to study the emission lines in more detail.

4.2. Companion galaxies

The cutout images of the QSO (Fig. 1) show two companions located $5''$ to the NE and $4''$ to the SW. According to the ALHAMBRA catalogue (Molino et al. 2013, in prep.), the NE source corresponds to an $AB(I) = 23.8$ blue galaxy at photometric redshift $z_{ph} = 2.25$ whose spectrum peaks at ≈ 6500 Å, and the SW source corresponds to an $AB(I) = 25.2$ blue galaxy at photometric redshift $z_{ph} = 2.10$ peaking at ≈ 5500 Å. The former has a counterpart in the NED database, the source RCS-01020502096 from the Red-Sequence Cluster Survey (Hsieh et al. 2005) with a reported redshift of 0.249. However, the R band magnitude of this object ($R = 23.6$) puts it well below the limit that Hsieh et al. (2005) quote for good quality redshifts in

their catalogue. No other counterpart has been found for the second source. According to our data both sources correspond to low-to-average mass galaxies ($\log(M/M_\odot) \approx 10.5 \sim 10.8$).

Given the estimated masses for the companions and their distance to the QSO, they should provide negligible gravitational lensing amplification to the quasar image (Willott et al. 2005). We have checked this for the observed configuration (including both redshift possibilities in the case of the NE source), establishing an upper limit to the possible magnification of 0.4%. This may not be exact as the colours of both sources are intrinsically blue and we have used a simple model of an early galaxy type halo—however, no realistic halo model would yield a significantly different result, not over a factor of two in the magnification effect (Bartelmann & Schneider 2001).

4.3. Black hole mass

The best black hole measurements (apart from reverberation mapping) can only be obtained using the FWHM of H β or MgII $\lambda 2800$ as a surrogate (Marziani & Sulentic 2012). Unfortunately, there is no currently available NIR spectra that covers the wavelength range where these lines are located (1.8 and 3.1 μm for MgII and H β respectively). Nevertheless, a crude estimation of the the black hole mass and bolometric luminosity can be obtained through the rest-frame 1350 Å continuum flux measurement. The observed 1350 Å continuum flux value of $(1.78 \pm 0.27) \times 10^{-18}$ erg s $^{-1}$ cm $^{-2}$ Å $^{-1}$ translates into an absolute luminosity of $(5.03 \pm 0.76) \times 10^{45}$ erg s $^{-1}$ at 1350 Å, assuming an isotropic emission and that the QSO flux has not been magnified by gravitational lensing. A bolometric luminosity of $(1.91 \pm 1.05) \times 10^{46}$ erg s $^{-1}$ was obtained following the prescription given in Richards et al. (2006a) (a 3.8 ± 2.0 factor at $\log(\nu) \approx 15.3$ Hz). A black hole mass of $(1.52 \pm 0.83) \times 10^8 M_\odot$ is derived assuming that the QSO is radiating at the Eddington limit (Peterson 1997). We note that a recent study of high-redshift quasars by Willott et al. (2010a) has shown that assumption to be reasonable, with all nine $z \approx 6$ quasars in their sample having $0.3 < L_{\text{Bol}}/L_{\text{Edd}} < 2.5$ and $\langle L_{\text{Bol}}/L_{\text{Edd}} \rangle = 1.3$.

4.4. Ancillary data

There is a detection of ALH023002+004647 by SDSS in the Stripe 82 coadd (SDSS J023002.28+004646.8) with reported magnitudes of 29.00 ± 1.45 , 26.62 ± 1.00 , 24.31 ± 0.18 , 22.64 ± 0.07 and 21.79 ± 0.10 in the u , g , r , i and z bands respectively. No optical, ultraviolet and radio detections by HST, GALEX, XMM-OM and VLA-FIRST are reported by MAST⁵ for ALH023002+004647. The Infrared Science Archive (IRSA⁶) provides counterparts above $5\text{-}\sigma$ from Spitzer/IRAC observations at 3.6, 4.5 and 5.8 μm with a $3.8''$ aperture flux of $9.56(\pm 0.36)$, $13.45(\pm 0.57)$ and $14.17(\pm 2.60)$ μJy , respectively. These fluxes are compatible, within the errors, with the photo- z best fit solution SED. The sky position of ALH023002+004647 is covered by the Field-4 of the DEEP2 Redshift Survey. Neither the discovered QSO nor the companions have spectroscopic information in the latest data release DR4 (Newman et al. 2012).

The cross-correlation of the ALH023002+004647 position with the high energy HEASARC⁷ and XSA⁸ databases reveals that the field has only been observed by XMM-Newton with the

⁵ <http://archive.stsci.edu/>

⁶ <http://irsa.ipac.caltech.edu>

⁷ <http://heasarc.gsfc.nasa.gov/>

⁸ <http://xmm.esac.esa.int/xsa/>

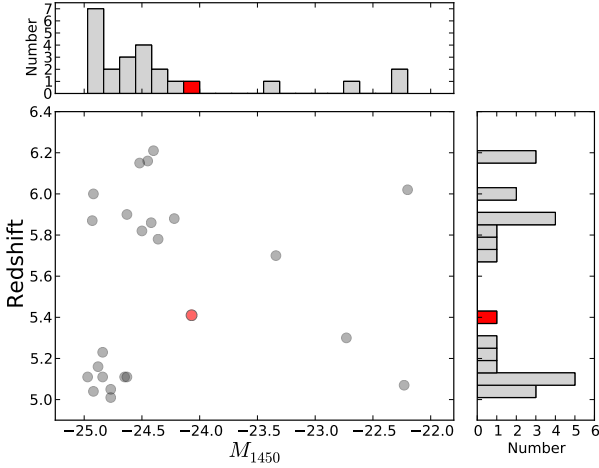


Fig. 3. Luminosity–redshift distribution for the 24 currently known faint ($M_{1450} > -25$) QSOs above $z = 5$. References for the 23 grey-filled circles are: Mahabal et al. (2005, 1 src), Jiang et al. (2009, 4 srcs), Willott et al. (2010b, 6 srcs), Masters et al. (2012, 2 srcs) and McGreer et al. (2012, 10 srcs). ALH023002+004647 is indicated by a red-filled circle and histograms.

Epic camera. We find no counterpart associated with the QSO as the closest *XMM-Newton* detection is located $12''$ from the QSO and coincides with a galaxy at $z = 0.73$.

5. Discussion

With $M_{1450} = -24.07 \pm 0.2$, ALH023002+004647 is the 5th (out of 24) less luminous QSOs known above redshift of $z = 5$. As a consequence, it samples the faint part ($M_{1450} > -25$) of QLF, which is currently poorly constrained at these redshifts. This is illustrated in Fig. 3 where we have plotted, in the redshift–luminosity space, all the faint spectroscopically confirmed QSO with $z > 5$. Stronger constraints to the space density of high- z low luminosity QSOs are needed to address questions as the implications for early AGN/host-galaxy interactions or the true fraction of ionizing photons coming from AGN activity in an epoch of increasing QSO activity and significant BH growth. Therefore, in the following we derive the space density associated with the ALH023002+004647 detection.

A first approximation to the contribution of ALH023002+004647 to the $z \approx 5.5$ space density has been computed using the binned $1/V_a$ method of Avni & Bahcall (1980), where V_a is the comoving volume per magnitude and redshift interval accessible to the source, taking into account the characteristics of the survey. It is defined as,

$$V_a = \int_{\Delta M} \int_{\Delta z} p(M, z) \frac{dV}{dz} dz dM,$$

where $p(M, z)$ is the function that corrects for the survey incompleteness at each M and z . The space density associated to ALH023002+004647 is computed as $\Phi(M, z) = 1/V_a$. The first release of the ALHAMBRA photometric database has been recently finalised and its completeness needs to be addressed through extensive simulations. So, for the time being, and given our first order approximation, we will consider that all “possible” type-I QSOs within the magnitude limits of the survey

could have been detected (i.e. $p(M, z) = 1$). We find this to be a reasonable assumption based on previous results for QSO completeness maps of similar surveys like COMBO-17 (see Fig. 4 in Wolf et al. 2003). Therefore, the volume accessible to our QSO is only delimited by the redshift range $z=[5.0, 6.1]$. At $z \sim 6.1$ the QSO would no longer satisfy our selection criteria, as the magnitude m_{830} would be fainter than ~ 25 when it samples the Ly-forest of the spectra. The lower limit redshift is fixed by our requirement to have a best fit model with $z_{PHOT} \geq 5.0$. The necessary K -corrections have been derived using the best-fit template for the photo- z solution. Considering the covered area ($\approx 1 \text{ deg}^2$) and the magnitude limit of our selection, we derive a space density of $(9.15^{+21.06}_{-9.15}) \times 10^{-8} \text{ Mpc}^{-3} \text{ mag}^{-1}$ for ALH023002+004647. The errors were estimated from Poisson statistics (Gehrels 1986). The result is presented in Figure 4. In order to illustrate the large uncertainties of the high- z QLF, we have delimited by a grey-shaded area the luminosity-density space covered by several published QLFs in the $z \sim 5 - 6$ redshift range, namely: CFQRS+SDSS-Deep (Willott et al. 2010b), SDSS-stripe82 (McGreer et al. 2012), COMBO-17 (Wolf et al. 2003) and SDSS-Deep-Stripe (Jiang et al. 2009). Two of the most recent determinations of the QLF at $z = 5$ (McGreer et al. 2012) and $z = 6$ (Willott et al. 2010b) are highlighted by the blue and black lines respectively. We also report the upper limits derived by Ikeda et al. (2012) from the non-detections of QSOs in the redshift bin $[4.5-5.5]$ of the COSMOS field (*black pentagons*) and the faintest QSO identification above $z = 5$ in the SXDS field (*black square*) as the only constraints to the very faint end of the QLF.

The associated error due to poor statistics hardly constrains the $z \sim 5-6$ QLFs, making our measurement compatible with all the previous, both single and double power-law, determinations. Nevertheless, the result is very promising considering that the QSO selection was made in a fraction of the total area covered by ALHAMBRA and based on preliminary photometry. With the final release of the ~ 4 sq. degrees of ALHAMBRA data already in place, our collaboration aims to further constraint the QLF over a much larger range of magnitudes and redshifts.

6. Conclusions

We report the discovery of ALH023002+004647, a new, intrinsically faint, QSO at $z = 5.41$. The candidate was selected based on a SED fitting to the 23 bands of the ALHAMBRA photometry and spectroscopically confirmed with GTC/OSIRIS. The observed continuum luminosity at 1450 \AA ($M_{1450} \sim -24$) and derived bolometric luminosity of $\approx 2 \times 10^{46} \text{ erg s}^{-1}$, makes ALH023002+004647 one of the faintest QSOs discovered above $z = 5$. Based on the ALH023002+004647 space density (and associated errors), no tighter constraints can be placed on the $z \sim 5 - 6$ QLF. Nonetheless, we have demonstrated the capabilities of the ALHAMBRA survey to select this type of sources. An analysis similar to the one presented here, applied to the final release of the ALHAMBRA photometric database (DR4) in the near future, will surely provide a significant contribution to the QLF at these very high redshifts.

Acknowledgements. Part of this work was supported by Junta de Andalucía, through grant TIC-114 and the Excellence Project P08-TIC-3531, and by the Spanish Ministry for Science and Innovation through grants AYA2006-1456, AYA2010-15169 and AYA2010-22111-C03-02, and Generalitat Valenciana project Prometeo 2008/132. IM thanks Cecile Cartozo for the careful reading of the manuscript. This research has made use of the NASA/IPAC Extragalactic Database (NED) which is operated by the Jet Propulsion Laboratory, California Institute of Technology, under contract with the National Aeronautics and Space

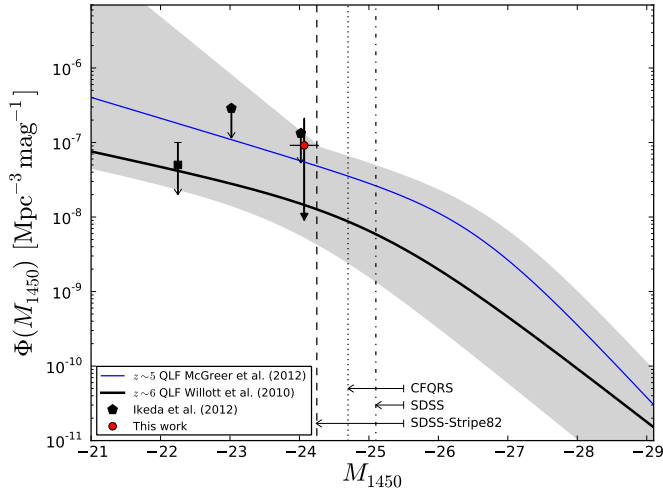


Fig. 4. QSO space density distribution as a function of the rest-frame 1450 Å monochromatic magnitude. The corresponding space density of ALH023002+004647 is represented by the red dot. For comparison with some recent determinations of the high- z QLF, we have plotted the $\langle z \rangle \sim 5$ SDSS-Stripe82 QLF derived by McGreer et al. (2012, *blue line*) and the $\langle z \rangle \sim 6$ CFQRS+SDSS-Deep QLF derived by Willott et al. (2010b, *black line*). The vertical lines indicate the faintest magnitude bin sampled by the SDSS-Main, SDSS-Stripe82 and CFQRS. The grey shaded area delimits the range covered by the published QLFs in the redshift bin [5-6] (see text for details). The *black pentagons* represent the upper limits derived by Ikeda et al. (2012) in the COSMOS field while the *black square* shows the space density associated to the faintest known QSO above $z = 5$ (Willott et al. 2010b).

Administration. Based on observations collected at the Centro Astronómico Hispano Alemán (CAHA) at Calar Alto, operated jointly by the Max-Planck Institut für Astronomie and the Instituto de Astrofísica de Andalucía (CSIC), and on observations made with the Gran Telescopio Canarias (GTC), installed in the Spanish Observatorio del Roque de los Muchachos of the Instituto de Astrofísica de Canarias, on the island of La Palma. MP acknowledges financial support from the JAE-Doc program of the Spanish National Research Council (CSIC), co-funded by the European Social Fund.

References

- Aparicio Villegas, T., Alfaro, E. J., Cabrera-Caño, J., et al. 2010, *AJ*, 139, 12421253
- Avni, Y. & Bahcall, J. N. 1980, *ApJ*, 235, 694
- Bartelmann, M. & Schneider, P. 2001, *Phys. Rep.*, 340, 291
- Benítez, N., Moles, M., Aguerri, J. A. L., et al. 2009, *ApJ*, 692, L5L8
- Bongiorno, A., Zamorani, G., Gavignaud, L., et al. 2007, *A&A*, 472, 443454
- Croom, S. M., Richards, G. T., Shanks, T., et al. 2009, *MNRAS*, 399, 17551772
- Croom, S. M., Smith, R. J., Boyle, B. J., et al. 2004, *MNRAS*, 349, 13971418
- Di Matteo, T., Springel, V., & Hernquist, L. 2005, *Nature*, 433, 604607
- Dunkley, J., Komatsu, E., Nolta, M. R., et al. 2009, *ApJS*, 180, 306
- Fan, X., Narayanan, V. K., Lupton, R. H., et al. 2001, *AJ*, 122, 28332849
- Fan, X., Strauss, M. A., Becker, R. H., et al. 2006, *AJ*, 132, 117136
- Fernández-Soto, A., Lanzetta, K. M., & Chen, H.-W. 2003, *MNRAS*, 342, 1215
- Gaskell, C. M. 1982, *ApJ*, 263, 79
- Gehrels, N. 1986, *ApJ*, 303, 336346
- Hopkins, P. F., Croton, D., Bundy, K., et al. 2010, *ApJ*, 724, 915945
- Hsieh, B. C., Yee, H. K. C., Lin, H., & Gladders, M. D. 2005, *ApJS*, 158, 161
- Ikeda, H., Nagao, T., Matsuoka, K., et al. 2012, *ApJ*, 756, 160
- Jiang, L., Fan, X., Bian, F., et al. 2009, *AJ*, 138, 305
- Khandai, N., Feng, Y., DeGraf, C., Di Matteo, T., & Croft, R. A. C. 2012, *MNRAS*, 423, 2397

- Mahabal, A., Stern, D., Bogosavljević, M., Djorgovski, S. G., & Thompson, D. 2005, *ApJ*, 634, L9
- Marziani, P. & Sulentic, J. W. 2012, *New A Rev.*, 56, 4963
- Masters, D., Capak, P., Salvato, M., et al. 2012, *ApJ*, 755, 169
- Matute, I., Márquez, I., Masegosa, J., et al. 2012, *A&A*, 542, A20
- McGreer, I. D., Jiang, L., Fan, X., et al. 2012, *ArXiv e-prints*
- Melia, F. 2013, *ApJ*, 764, 72
- Moles, M., Benítez, N., Aguerri, J. A. L., et al. 2008, *AJ*, 136, 13251339
- Newman, J. A., Cooper, M. C., Davis, M., et al. 2012, *ArXiv e-prints*
- Palanque-Delabrouille, N., Magneville, C., Yèche, C., et al. 2013, *A&A*, 551, A29
- Pâris, I., Petitjean, P., Aubourg, É., et al. 2012, *A&A*, 548, A66
- Peterson, B. M. 1997, *An Introduction to Active Galactic Nuclei*
- Richards, G. T., Fan, X., Newberg, H. J., et al. 2002a, *AJ*, 123, 29452975
- Richards, G. T., Lacy, M., Storrie-Lombardi, L. J., et al. 2006a, *ApJS*, 166, 470497
- Richards, G. T., Strauss, M. A., Fan, X., et al. 2006b, *AJ*, 131, 2766
- Richards, G. T., Vanden Berk, D. E., Reichard, T. A., et al. 2002b, *AJ*, 124, 1
- Ross, N. P., McGreer, I. D., White, M., et al. 2012, *ArXiv e-prints*
- Schroeder, J., Mesinger, A., & Haiman, Z. 2013, *MNRAS*, 428, 3058
- Shen, Y., Strauss, M. A., Oguri, M., et al. 2007, *AJ*, 133, 2222
- Siana, B., Polletta, M. d. C., Smith, H. E., et al. 2008, *ApJ*, 675, 49
- Willott, C. J., Albert, L., Arzoumanian, D., et al. 2010a, *AJ*, 140, 546560
- Willott, C. J., Delorme, P., Reylé, C., et al. 2010b, *AJ*, 139, 906918
- Willott, C. J., Percival, W. J., McLure, R. J., et al. 2005, *ApJ*, 626, 657
- Wolf, C., Wisotzki, L., Borch, A., et al. 2003, *A&A*, 408, 499514